Peptide functionalized poly ethylene glycol-poly caprolactone nanomicelles for specific cabazitaxel delivery to metastatic breast cancer cells

By: Mandaviani, P (Mandaviani, Parvin)[1,2]; Bahadorikhalili, S (Bahadorikhalili, Saeed)[3]; Navaei-Nigjeh, M (Navaei-Nigjeh, Mona)[4,5]; Vafaei, SY (Vafaei, Seyed Yaser)[1]; Esfandyari-Manesh, M (Esfandyari-Manesh, Mehdi)[2]; Abdolghaffari, AH (Abdolghaffari, Amir Hossein)[5,6]; Daman, Z (Daman, Zahra)[1]; Atyabi, F (Atyabi, Fatemeh)[1,2]; Ghahremani, MH (Ghahremani, Mohammad Hossein)[7]; Amini, M (Amini, Mohsen)[8,10] ...More

View ResearcherID and ORCID

MATERIALS SCIENCE & ENGINEERIN

Volume: 80 **Pages:** 301-312

DOI: 10.1016/j.msec.2017.05.126

Published: NOV 1 2017

View Journal Impact

Abstract

Metastatic cancer is responsible for 90% delivery and efficacy of chemotherapeut surface of nano-carriers with various tar efficacy. Using specified peptides in targ study, tumor metastasis targeting (TMT) specific drug delivery to tumor cells. TM caprolactone (PEG-PCL) micellar nanop metastatic breast cancer cells. Synthesi between carboxylic acid group of PEG a solvent evaporation method. TMT peptic amine group of PEG. TMT-PEG-PCL na spectroscopy (FTIR), scanning electron permeation chromatography (GPC) and uptake of nanomicelles were investigate microscopy in MCF-7 (non-metastatic breast cancer cells) and MDA-MB-231 (metastatic breast cancer cells). The final nanomicelles had about 110 nm mean size and encapsulation efficiency of 82.5%. Treatment of metastatic breast cancer cells with targeted nanomicelles significantly increased the necrosis rate to 65%, compared to 33% in non-targeted nanomicelles and 8% in control group. The MDA-MB-231 cells treated with targeted nanomicelles exhibited a strong increase in the fluorescence intensity of coumarin in comparison to the cells treated with non-targeted nanomicelles ($p < 0.001$). It could be concluded that the present carrier has the potential to be considered in treatment of metastatic breast cancer cells. (C) 2017 Elsevier B.V. All rights reserved.

Keywords

Author Keywords: Homing peptide; Cabazitaxel; Nanomicelles; Metastatic breast cancer; Necrosis

KeyWords Plus: RESISTANT PROSTATE-CANCER; TARGETED DRUG-DELIVERY; POORLY SOLUBLE DRUGS; POLYMERIC MICELLES; TUMOR VASCULATURE; POLY(ETHYLENE OXIDE)-

B-POLY(EPSILON-CAPROLACTONE); BLOCK-COPOLYMER; NANOPARTICLES; INHIBITION; PACLITAXEL

Author Information

Reprint Address: Dinarvand, R (reprint author)

+ Univ Tehran Med Sci, Fac Pharm, Tehran 1417614411, Iran.

Addresses:

+ [1] Univ Tehran Med Sci, Fac Pharm, Dept Pharmaceut, Tehran, Iran
+ [2] Univ Tehran Med Sci, Fac Pharm, Nanotechnol Res Ctr, Tehran, Iran
+ [3] Univ Tehran, Sch Chem, Coll Sci, Tehran, Iran
+ [4] Univ Tehran Med Sci, Sch Adv Technol Med, Dept Tissue Engn & Appl Cell Sci, Tehran, Iran
+ [5] Univ Tehran Med Sci, Pharmaceut Sci Res Ctr, Toxicol & Dis Grp, Tehran, Iran
+ [6] ACECR, Inst Med Plants, Med Plants Res Ctr, Karaj, Iran
+ [7] Univ Tehran Med Sci, Fac Pharm, Dept Pharmacol & Toxicol, Tehran, Iran
+ [8] Univ Tehran Med Sci, Fac Pharm, Dept Med Chem, Tehran, Iran
+ [9] Univ Alberta, Fac Pharm & Pharmaceut Sci, Edmonton, AB T6G 2E1, Canada
+ [10] Univ Tehran Med Sci, Drug Design & Dev Res Ctr, Tehran, Iran

E-mail Addresses: dinarvand@tums.ac.ir

Funding

Funding Agency	Grant Number
Tehran University of Medical Sciences	9201-57-22033

View funding text

Publisher

ELSEVIER SCIENCE BV, PO BOX 211, 1000 AE AMSTERDAM, NETHERLANDS

Categories / Classification

Research Areas: Materials Science

Web of Science Categories: Materials Science, Biomaterials

Document Information

Document Type: Article

Language: English

Accession Number: WOS:000410254400037

PubMed ID: 28866169

ISSN: 0928-4931

eISSN: 1873-0191

Journal Information

Impact Factor: Journal Citation Reports

Other Information

IDS Number: FG4RY

Cited References in Web of Science Core Collection: 32

Times Cited in Web of Science Core Collection: 0

Materials Science and Engineering C 80 (2017) 301–312

Contents lists available at ScienceDirect

Materials Science and Engineering C

journal homepage: www.elsevier.com/locate/msec

Peptide functionalized poly ethylene glycol-poly caprolactone nanomicelles for specific cabazitaxel delivery to metastatic breast cancer cells

Parvin Mahdaviani [a,b], Saeed Bahadorikhalili [c], Mona Navaei-Nigjeh [d,e], Seyed Yaser Vafaei [a], Mehdi Esfandyari-Manesh [b], Amir Hossein Abdolghaffari [f,e], Zahra Daman [a], Fatemeh Atyabi [a,b], Mohammad Hossein Ghahremani [g], Mohsen Amini [h,j], Afsaneh Lavasanifar [i], Rassoul Dinarvand [a,b,*]

[a] Department of Pharmaceutics, Faculty of Pharmacy, Tehran University of Medical Sciences, Tehran, Iran
[b] Nanotechnology Research Center, Faculty of Pharmacy, Tehran University of Medical Sciences, Tehran, Iran
[c] School of Chemistry, College of Science, University of Tehran, Tehran, Iran
[d] Department of Tissue Engineering and Applied Cell Sciences, School of Advanced Technologies in Medicine, Tehran University of Medical Sciences, Tehran, Iran
[e] Toxicology and Diseases Group, Pharmaceutical Sciences Research Center, Tehran University of Medical Sciences, Tehran, Iran
[f] Medicinal Plants Research Center, Institute of Medicinal Plants, ACECR, Karaj, Iran
[g] Department of Pharmacology and Toxicology, Faculty of Pharmacy, Tehran University of Medical Sciences, Tehran, Iran
[h] Department of Medicinal Chemistry, Faculty of Pharmacy, Tehran University of Medical Sciences, Tehran, Iran
[i] Faculty of Pharmacy and Pharmaceutical Sciences, University of Alberta, Edmonton, AB T6G 2E1, Canada
[j] Drug Design and Development Research Center, Tehran University of Medical Sciences, Tehran, Iran

ARTICLE INFO

Article history:
Received 9 November 2016
Received in revised form 16 May 2017
Accepted 17 May 2017
Available online 20 May 2017

Keywords:
Homing peptide
Cabazitaxel
Nanomicelles
Metastatic breast cancer
Necrosis

ABSTRACT

Metastatic cancer is responsible for 90% of deaths in world. Usage of nano-carriers improve the delivery and efficacy of chemotherapeutic agents. Recent studies suggest that decoration of the surface of nano-carriers with various targeting agents may further improve their overall therapeutic efficacy. Using specified peptides in targeted drug delivery is a key point in recent researches. In this study, tumor metastasis targeting (TMT) homing peptide was applied as a targeting group to improve specific drug delivery to tumor cells. TMT peptide is conjugated to poly ethylene glycol-poly caprolactone (PEG-PCL) micellar nanoparticles as carriers for targeted delivery of cabazitaxel to metastatic breast cancer cells. Synthesis of PEG-PCL copolymer was performed by amidation reaction between carboxylic acid group of PEG and amine group of PCL. Nanomicelles were prepared via solvent evaporation method. TMT peptide was covalently conjugated onto nanomicelles through the amine group of PEG. TMT-PEG-PCL nanoparticles were analyzed by Fourier transform infrared spectroscopy (FTIR), scanning electron microscope (SEM), dynamic light scattering (DLS), gel permeation chromatography (GPC) and nuclear magnetic resonance (NMR). Toxicity and cellular uptake of nanomicelles were investigated by in vitro cytotoxicity assays and confocal scanning microscopy in MCF-7 (non-metastatic breast cancer cells) and MDA-MB-231 (metastatic breast cancer cells). The final nanomicelles had about 110 nm mean size and encapsulation efficiency of 82.5%. Treatment of metastatic breast cancer cells with targeted nanomicelles significantly increased the necrosis rate to 65%, compared to 33% in non-targeted nanomicelles and 8% in control group. The MDA-MB-231 cells treated with targeted nanomicelles exhibited a strong increase in the fluorescence intensity of coumarin in comparison to the cells treated with non-targeted nanomicelles ($p < 0.001$). It could be concluded that the present carrier has the potential to be considered in treatment of metastatic breast cancer cells.

1. Introduction

Cabazitaxel (CBZ) is a semi-synthetic derivative of a natural toxoid, which is commercially applied for treatment of patients with hormone-refractory metastatic prostate cancer previously treated with a docetaxel-containing regimen. Previous studies showed that CBZ has antitumor activity against both docetaxel-sensitive and docetaxel-insensitive tumor models. A challenging drawback of CBZ is its poor water solubility, due to its bulky polycyclic structure. Tween 80 and ethanol has been used in CBZ formulation to increase its solubility which may cause severe side effects such as hypersensitivity and neurotoxicity [1,2]. An advantageous approach for overcoming this problem is the use of nanoparticles (NPs)

* Corresponding author at: Faculty of Pharmacy, Tehran University of Medical Sciences, Tehran 1417614411, Iran.
E-mail address: dinarvand@tums.ac.ir (R. Dinarvand).

http://dx.doi.org/10.1016/j.msec.2017.05.126
0928-4931/

containing encapsulated, dispersed, absorbed or conjugated drugs. NPs have unique characteristics which can lead to increase therapeutic index of chemotherapeutic drugs [3]. This outcome is mainly owed to the preferred localization of anti-cancer drugs in tumor by NPs. Nanocarriers such as liposomes and micelles show improvement in pharmaceutical properties of commercially available traditional formulations. NPs with hydrophilic surfaces can avoid opsonization and removal by the mononuclear phagocytic cells, stay away from extravasation through the continuous capillaries of healthy tissues and escape filtration by kidneys [4]. NPs with size between 50 and 150 nm can utilize the angiogenic vasculature of tumors for accumulation into tumor sites. Because of poor lymphatic drainage at tumor sites, results in a phenomenon known as the enhanced permeability and retention (EPR) effect [4]. Between different drug delivery systems, polymeric micelles are include of a hydrophilic shells which most of time is polyethylene glycol and a hydrophobic core that is reservoir for hydrophobic chemotherapeutic drugs such as CBZ [4,5]. Polymeric micelles (PMs) are spherical, nano-sized (10–200 nm) aggregates of amphiphilic copolymers that can be used as a delivery agent for breast cancer chemotherapy. PMs show different advantages over traditional drug delivery systems such as: Easy intravenous administration by increment of hydrophobic drugs solubility [6]. The hydrophilic micellar corona, in turn, forms a hydrating layer on the surface of the micelle that hinders plasma protein adsorption and subsequent rapid phagocytic clearance by the reticuloendothelial system (RES) [7]. PMs have notable potential for modifications, in which additional functional groups can be attached to the surface and used to modulate micelle properties. Particularly, the addition of a targeting ligand can increase the specificity of drug delivery to tumors [8]. They show low critical micelle concentrations (CMCs) attributing to small micellar size resulting in long-circulating and stable constructs [9].

Decorating the drug carrier with tumor cell can be facilitating the uptake of the drugs into the cells. This molecules will result in [1] higher retention of the drug carriers at tumor sites (i.e., by reducing passive transport away from tumor); and [2] improve uptake of the drugs by tumor cells.

Targeted delivery of the drugs is an approach for both increasing the efficiency and decreasing the side effects, especially for anticancer drug delivery [10]. Among different targeting strategies, antibodies are used as tumor-binding ligands, but a more fruitful approach is to utilize tumor specific peptides. The smaller size of peptides allows for better tumor penetration. In addition, the technology of peptide chemistry and engineering is more amenable for drug development. Tumor targeting with peptide ligands for cancer imaging and therapy has been extensively evaluated [11].

Peptide-mediated targeted therapy is achieved either through direct conjugation of an anti-cancer drug to peptide ligands or through preparation of peptide-guided drug carriers. Compared to peptide-drug conjugates, carriers bearing multiple tumor targeting peptides display increased affinity for cancer cells overexpressing the appropriate receptors, show better pharmacokinetics/tumor accumulation and are more likely to be internalized via receptor mediated endocytosis [12–15].

A cyclic ten-amino acid peptide (GCGNVVRQGC), referred to tumor metastasis targeting (TMT) peptide, is the ligand of XPNPEPZ, a subtype of aminopeptidase P. TMT peptide has been found to specifically bind to a series of highly metastatic tumor, such as PC-3M-1E8, MDA-MB-435S, MDA-MB-231, PG-BE1 and MKN-45sci, in vitro and in vivo, but not to the non-metastatic cell lines (such as PC-3M-2B4, MCF-7, PG-LH7 and NIH/3T3). This actually offers one potential avenue for developing nanocarriers that can specifically target and treat metastatic cancer [15,16].

As mentioned, CBZ is a commercial anticancer drug and is intensely attracted interests, due to outstanding properties such as high activity against both docetaxel-sensitive and docetaxel-insensitive tumor models [17]. This drug, but suffers the lack of solubility, which can be improved by loading on amphiphilic nanoparticles. Therefore, in this study we introduce PEG-PCL micelles for CBZ delivery. Moreover, TMT was used for more efficient targeting delivery. TMT efficaciously and selectively binds to metastatic tumor cells. In this study, we prepared a nanocarrier micelle system based on PEG-PCL. PEG-PCL micelles will improve the solubility problem of CBZ. TMT Homing peptide was conjugated to the surface of the NPs for promoting efficient and active targeting of the anticancer CBZ. In vitro delivery efficiency of the CBZ loaded TMT modified NPs was evaluated by comparing the cytotoxicity and cellular uptake of non-targeted and peptide-targeted formulations in MDA-MB-231 (metastatic breast cancer) cell line and MCF-7 (non-metastatic breast cancer) cells.

2. Materials and methods

2.1. Materials, cell lines

NH_2-PEG-COOH (Mw = 5000 Da), ε-caprolactone (ε-CL), stannousoctoate ($Sn(Oct)_2$) were purchased from Sigma-Aldrich Chemical Corp. (Shanghai, China); Cabazitaxel was supplied by the Shanghai Institute of Pharmaceutical Industry (Shanghai, China). Dulbecco's Modified Eagle Medium (DMEM) High Glucose was purchased from Hy Clone Thermo Scientific. Fetal Bovine Serum (FBS) was purchased from Gibco-Life Technologies. Penicillin/streptomycin and 0.25% (w/v) trypsin–0.1% (w/v) Ethylene Diamine Tetraacetic Acid (EDTA) were purchased from Solarbio (Beijing Solarbio Science and Technology, China). 3-(4, 5-dimethyl-thiazol-2-yl)-2, 5-diphenyl-tetrazolium bromide (MTT) and dimethylsulfoxide (DMSO) were purchased from sigma (USA). Culture flasks and dishes were from Corning (Corning, NY, USA). HPLC-grade acetonitrile was purchased from Anaqua Chemical Supply (Houston, TX, USA). Ethanol absolute, Tween 80, ammonium acetate of AR grade and spectrographic grade potassium bromide (KBr) were obtained from Sinopharm Chemical Reagent Co., Ltd. (Shanghai, China). All other chemicals were of analytical reagent grade and purchased from commercial sources.

The metastatic breast cancer cell lineMDA-MB-231 and non-metastatic breast cancer cell line MCF-7 obtained from American Type Culture Collection (Manassas, VA) and cultured in RPMI-1640 and DMEM media respectively supplemented with 10% fetal bovine serum (FBS), penicillin (100 U mL^{-1}), streptomycin (100 μg mL^{-1}) at 37 °C in a humidified incubator supplemented with 5% carbon dioxide.

2.2. Preparation of nanocarrier, Boc-protection of amine group

Amino end of poly (ethylene glycol) 2-aminoethyl ether acetic acid (Mn = 5000D) and 3-aminopropan-1-ol were separately protected by di-tert-butyl dicarbonate (Boc_2O) according to the previously reported procedures. To a magnetically stirred mixture of amine (2 mmol) and $(Boc)_2O$ (2 mmol, 1 equiv) in a 25 mL round bottom flask, was added pyridine (80microlit) and the mixture was stirred at room temperature (30–35 °C) until completion of the reaction (24 h). The reaction mixture was extracted with Ethyl acetate (3 × 5 mL). The solvent was evaporated and the product was washed out with Et_2O. The Boced product was obtained as a solid (95%), characterized by NMR and FT-IR [18].

2.3. Polymerization of ε-caprolactone

N-protected 3-aminopropan-1-ol was used as initiator for ring opening polymerization of ε-caprolactone. Synthesis was carried out in a three-necked round bottomed flask (100 mL) equipped with a thermometer, a condenser and magnetic stirrer. The flask was purged with argon, evacuated twice and stored under an inert atmosphere. Argon was blown through the water absorption system with silica gel. A mixture of N-Boced 3-aminopropan-1-ol (0.9 cm^3) and $Sn(Oct)_2$ (90 μL) was added to toluene at 90 °C and stirred for 30 min. The ε-caprolactone (8.9 cm^3) monomer was added to the reaction mixture and stirring continued at 110 °C for 24 h. The reaction temperature was maintained using a silicone oil bath. The polymer was precipitated by the addition

of cold methanol (polymer solution/methanol: 1/10) and dried at 45 °C under vacuum for 24 h. Trifluoroacetic acid was utilized for deprotection of the obtained product [18].

2.4. Synthesis of PEG-PCL copolymer

Synthesis of PEG-PCL copolymer was performed by amidation reaction between carboxylic acid group of PCL and amine end of PEG. To do this, Boc-PEG (1 mmol) was dissolved in dry dichloromethane followed by the addition of 1.2 mmol EDC and after 4 h 2.5 mmol NHS. The mixture was then stirred at room temperature to activate the carboxylic group of PEG. Subsequently, PCL (1 mol) was added to the above solution, and the mixture was stirred for 24 h at room temperature. The product was purified by dialysis using dialysis bag (Mw cut-off = 12 kDa). The product was deboced by trifluoroacetic acid, dried at reduced pressure and stored at 4 °C [18].

2.5. Preparation of micelle encapsulated cabazitaxel

A cosolvent evaporation method was used for the self-assembly of PEG/PCL copolymer and drug encapsulation. The ratio of organic to the aqueous phase and the order of addition of the phases in the cosolvent evaporation method were changed to optimize the preparation method in terms of carrier size and encapsulation efficiency. Optimized (D/P) ratios was 10% (w/w). Solvent evaporation procedure involved the dissolution of CBZ and PEG–PCL in acetone and dropwise addition of the mixture to MilliQ water under sonication by a Hielscher device (model UP400S, Hielscher ultrasound technology, Germany) with an output power of 50 W for 2 min, followed by the solvent elimination by a rotary vacuum evaporator (BuchiRotavapor R-124, Buchi, Switzerland). Finally, solution placed within a dialysis bag (Mw cut-off = 12 kDa), and dialyzed against deionized water overnight at room temperature. After dialysis, the micellar solution was centrifuged at 16,000 rpm for 5 min and the supernatant was collected. Finally, the resultant micellar formulations were filtrated through a 0.2 mm Minisart1 syringe filter, and immediately investigated in terms of size, zeta potential and loading characteristics. NPs filtered through a 0.45 mm Minisart syringe filter (Sartorius, Germany) to remove free cabazitaxel and subsequently lyophilized. Fluorescent coumarin 6 (10 mg/mL) loaded mixed micelle formulation were also prepared in the same way [18].

2.6. Conjugation of TMT peptide to PEG-PCL

TMT peptide was covalently conjugated onto PEG-PCL micelles through the —COOH group of the prepared PEG-PCL. To do this, Moc protected TMT peptide was attached to PEG-PCL using EDC and NHS. 0.2 mmol TMT was reacted with PEG-PCL using EDC and NHS according to the previous step procedure [18–22].

2.7. Determination of particle size and zeta potential

The hydrodynamic diameters of blank micelles and CBZ-loaded micelles were determined using a Malvern Zetasizer Nano ZS (Malvern Instruments Ltd., MA). Lyophilized sample (1 mg) was dissolved in 1 mL of water and filtered through a 0.2 μm PTFE filter prior to measurement. The zeta potential was determined using the same equipment, but lyophilized samples were dissolved in PBS (pH 7.4, 10 mM) at a final concentration of 1 mg/mL.

2.8. Drug loading parameters

To determine the concentration of CBZ, the lyophilized CBZ-loaded micelles were dissolved in acetonitrile and subjected to HPLC analysis using an Agilent 1260 Infinity Quaternary Liquid Chromatographic System with an UV detector operated at 248 nm and an Aglient ZORBAX Eclipse Plus C18 column (5 μm, 4.6 mm × 150 mm). The mobile phase was methanol. The flow rate was 1 mL/min. The drug loading and the entrapment efficiency were calculated using the following equations:

$$\text{Percent of drug loading } (\%) = (\text{Amount of drug in micelles})/(\text{initial amount of drug in system})$$

$$\text{Entrapment efficiency } (\%) = (\text{Amount of drug in micelles})/(\text{amount of micelles-free drug})$$

where (polymer weight + CBZ loaded amount) was approximately considered as the total nanoparticle weight [18].

2.9. Polymeric micelle morphology

The morphology and possible aggregation of the micelles was characterized using scanning electron microscopy (SEM) (Philips, model XL30, The Netherlands). For SEM imaging, freeze-dried polymeric micelle were placed on a stub, sputter coated with gold and evaluated at 30 kV using a 6300 field emission scanning electron microscope [18].

2.10. In vitro drug release

Drug release was studied in phosphate buffered saline medium (PBS; pH 7.4). Briefly, 35 mg of freeze-dried CBZ loaded PM at targeted and non-targeted formulation was dispersed in the medium and placed into dialysis bag (MW cut off 12 kDa, Sigma-Aldrich GmbH, Germany). The dialysis bag was incubated in 50 mL of PBS at 37 °C and shaken at 100 cycles/min. At the predetermined time intervals, 2 mL of the medium was collected for CBZ analysis by HPLC and equivalent volume of fresh PBS solution was supplemented in order to keep the volume of the system identical [23,24].

2.11. In vitro cytotoxicity assay

The cytotoxicity of free CBZ and CBZ encapsulated in NANO-PEG-PCL and NANO-TMT-PEG-PCL block copolymer micelles against different cell lines (MDA-MB-231, and MCF-7) was investigated using 3-(4,5-dimethylthiazol-2-yl)-2,5-diphenyltetrazolium bromide (MTT) assay. The cells were grown in the corresponding complete growth media and maintained at 37 °C with 5% CO_2 in a tissue culture incubator. Growth medium containing 8000 cells (4000 cells in case of the MDA-MB-231 cells) was placed in each well of a 96 well plate and incubated overnight to allow cell attachment. After 48 h when the cells had adhered (70% confluency), micellar solutions and free CBZ at 100 μM were incubated with the cells for 72 h. Control cells were cultured simultaneously in basic medium (DMEM containing 10% FBS and 1% antibiotic penicillin/streptomycin) without CBZ for the same time period.

Furthermore, the biocompatibility of copolymer micelles were assessed by treated of cells with NANO-PEG-PCL without CBZ.

MTT solution (50 μL; 5 mg/mL in double distilled water) was added to each well and the plates were incubated for a further 3–4 h. The media was aspirated and the formazan crystals were dissolved in DMSO. The plates were kept on an orbital shaker for 10 min and optical density was read on a multi-well scanning spectrophotometer (ELISA reader) at 570 nm. The viability of the treatment groups was expressed as the percentage of control which put on 100%. The mean and the standard error of mean (SEM) of cell viability for each treatment was determined.

2.12. Scratch wound healing study, in vitro wound healing assay

The effect of different preparations free CBZ, NANO-PEG-PCL, NANO-PEG-PCL-CBZ, and NANO-TMT-PEG-PCL-CBZ on cell migration was assessed by a scratch wound assay as described by Liang et al. with minor modifications. Briefly, cells were seeded in a 24 wells-plates and allowed to adhere overnight. The following day, cells were starved

in 0.1% FBS medium for 2 h and a vertical, uninterrupted wound was created in the cell monolayer using a sterile 10 μL pipette tip. Different polymeric micelles with and without CBZ and peptide ligands ((Different polymeric micelles with and without CBZ) CBZ loaded polymeric micelles) were added and incubated with MDA-MB-231 and MCF-7cells for 48 h at 37 °C. The final CBZ and polymer concentration in each well was 100 μM. Cells incubated with the medium were used as negative controls. Images of the wounded cell monolayer were taken using a Nikon Eclipse Te-2000-U microscope (4× magnification) at the start of the incubations and again after 48 h. The surface of the scratch area (A) was measured using Image J software. Results are expressed as percentages of wound area for each well using the formula: 100 × (At48 / At0). Statistical analysis was performed with Sigma Plot software using a one-way analysis of variance (ANOVA) followed by Student's *t*-test.

2.13. Cellular apoptosis assay

The analysis of apoptosis and necrosis induced by different preparations was determined after Annexin V FITC/PI double staining according to the manufacturer's protocols (Annexin V-FITC Apoptosis Detection Kit, Key Gen biotech, China). Briefly, MDA-MB-231 and MCF-7 cells were treated with NANO-PEG-PCL-CBZ, NANO-TMT-PEG-PCL-CBZ (containing100μMCBZ), or DMSO (vehicle control) for 48 h. By the end of the treatment, cells were harvested, washed with cold PBS, suspended in 500 μL binding buffer and stained by 5 μL Annexin V-FITC and 5 μL PI. The cells were incubated in the dark for 15 min and then measured by flowcytometer (Cytomics™ FC 500, Beckman Coulter, Miami, FL, USA).

2.14. In vitro cellular uptake studies

A confocal fluorescent microscope was used to compare the cellular uptake and intracellular distribution of micelles incubated with different cell lines. Briefly, MCF-7 and MDA-MB-231were grown on coverslips for 24 h till total adhesion and then incubated with NANO-PEG-PCL-coumarine-6, and NANO-TMT-PEG-PCL-coumarine-6 diluted in culture medium at 37 °C for 2 h. The cells were then washed three times with PBS, fixed with 4% paraformaldehyde in PBS at room temperature for 10 min, followed by cell nuclei staining with DAPI for 15 min. Finally, the cells were imaged by a laser scanning confocal microscope (Leica, Heidelberg, Germany). In addition, the total fluorescence signal per image (sum of green values of all pixels) was divided by the number of cell nuclei, to give the average fluorescence intensity of coumarin-6per cell [25].

3. Results

3.1. Synthesis of PEG-PCL copolymer

FT-IR and ^{1}HNMR were used to characterize the obtained PEG-PCL copolymers. The typical FT-IR spectrum is shown in Fig. 1. In Fig. 1a, FT-IR spectra of Boc-PEG reveals a band at 1103 cm^{-1} which is related to the C—O bond (PEG segment), and the peak at 2881 cm^{-1} results from the methylene group. In Fig. 1b, the absorption band at 1687 cm^{-1} is attributed to C═O stretching vibrations of the amide carbonyl group. The absorption bands at 1109 cm^{-1} is attributed to the characteristic C—O—C stretching vibrations of repeated —OCH_2CH_2 units, which proves the presence of PEG in the structure of the product. The absorption band at 3544 cm^{-1} is assigned to terminal hydroxyl groups in the copolymer. It is obvious in Fig. 1c that peptide-PEG-PCL copolymer exhibits characteristic peaks of both PEG and PCL segments. A peak at 2913 cm^{-1} is attributed to Moc protecting groups of TMT peptide. To further confirm the formation of peptide-PEG-PCL copolymer, ^{1}HNMR spectrum was also recorded and shown in Fig. 2. The characteristic absorption peaks were also indicated in this figure. Peaks at 1.40, 1.58, 1.69, 2.51, and 4.06 ppm are assigned to methylene protons of —$(CH_2)_3$—, —$OCCH_2$—, and —CH_2OOC— in PCL units, respectively. The peak at 3.61 ppm is attributed to methylene protons of —CH_2CH_2O in PEG units in block copolymer. By comparing the peak area correlated to the methylene groups of PEG by those of PCL, a 1:1 ratio of PEG to PCL can be observed. The molecular weight determined by GPC were 45,000 g mol^{-1}. Gel permeation chromatography (GPC) was used for the determination of the molecular weight of the PCL. As can be seen in Fig. 3, the molecular weight determined by GPC were 45,000 g mol^{-1}.

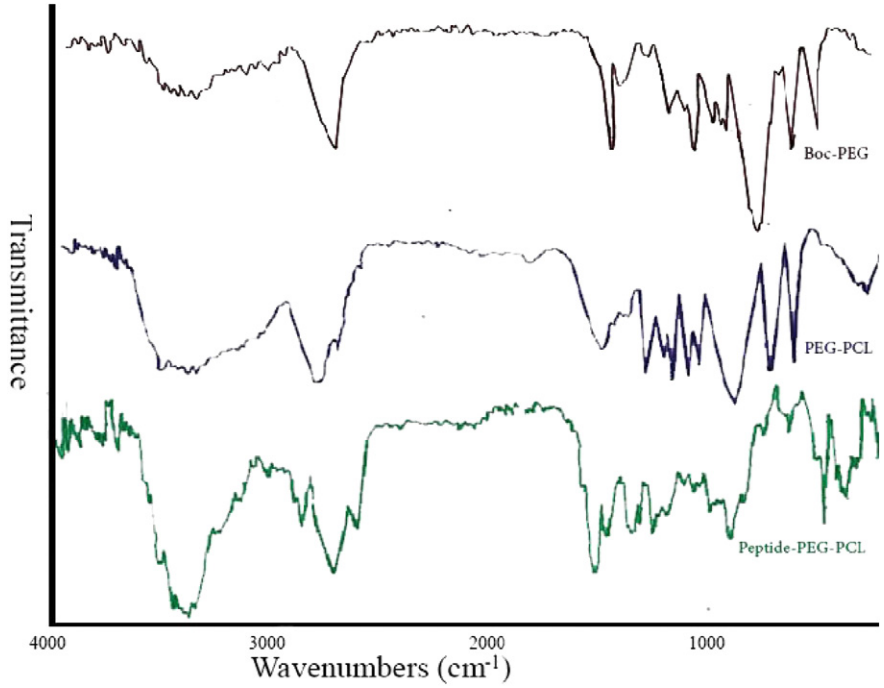

Fig. 1. The FTIR spectra of (a) PEG, (b) PEG-PCL, (c) Peptide-PEG-PCL.

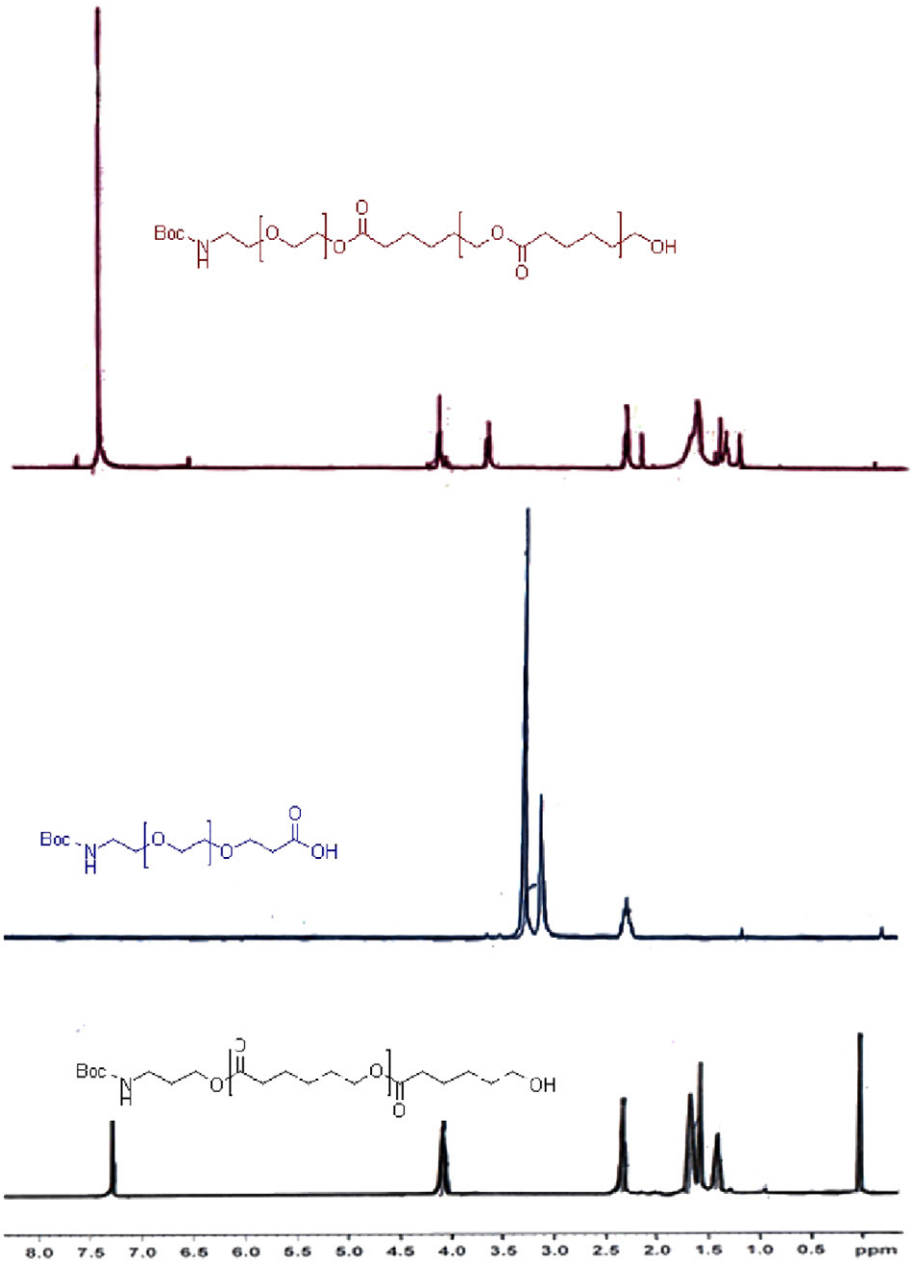

Fig. 2. ^{1}HNMR spectrum of (a) PEG-PCL, (b) PEG. (c) PCL.

3.2. Characterization of CBZ-PM

The average size of CBZ-PM obtained in this study was (110 ± 4.1) nm, with a PDI of 0.38 ± 0.045. The particle size had a unimodal distribution. Thus, it is beneficial to supply a prolonged pharmacological profile in vivo.

As can be seen in Fig. 4, The SEM image revealed that CBZ-PM was spherical and homogeneous and the average particle size was about 100 nm with a narrow particle size range. To our knowledge, SEM determine the size of dry particles, while the DLS determines the hydrodynamic diameter of particles in water. Because amphiphilic block polymeric micelles have a loose structure in water, the particle size determined by DLS was always slightly larger than that determined by SEM.

In addition, the DL and EE of CBZ-PM determined by validated HPLC method was 8.5% and 82.5%, respectively. Remarkably, the aqueous solubility of CBZ was increased by hundreds-fold after being encapsulated into the micelle, and higher EE would increase drug content at the site of action.

3.3. In vitro drug release behavior

To investigate the drug release behavior of free CBZ and CBZ-PM in vitro, a modified dialysis method was employed. As illustrated in Fig. 5, CBZ-PM showed a much slower cumulative release rate compared with the fast release profile of free CBZ. More than 95% of the CBZ was released to the medium in free CBZ group within 24 h, whereas only about 50% of the encapsulated CBZ was released from CBZ-PM. In a three day period, the cumulative release rate in CBZ-PM group was just 82% ± 3.05%.

3.4. In vitro cytotoxicity study

The effect of free CBZ, CBZ encapsulated in NANO-PEG-PCL and NANO-TMT-PEG-PCL, and NANO-PEG-PCL block copolymer micelles alone in both MCF-7 and MDA-MB-231 cells after 72 h incubation was evaluated using the MTT assay (Fig. 6).

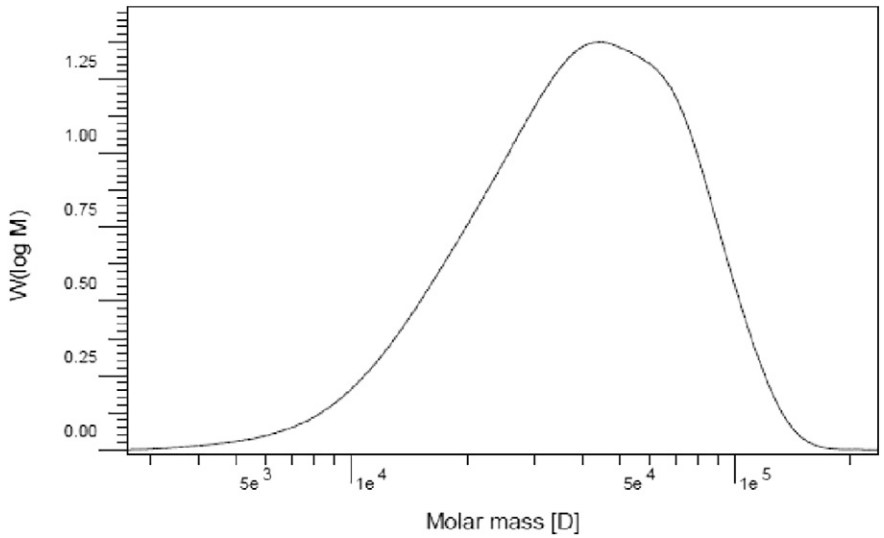

Fig. 3. GPC chromatogram of PCL.

Cell viability was compared with untreated control. The proliferation of both cells was inhibited when treated with free CBZ under this study ($p < 0.001$). Using encapsulated CBZ could also decrease the viability of cells which is significant in MDA-MB-231 cells in both targeted and non-targeted copolymer micelles ($p < 0.01$ and $p < 0.001$, respectively). In addition, the results showed that NANO-PEG-PCL alone has virtually no significant antitumor effects in both MCF-7 and MDA-MB-231 cells.

Further, the antitumor activity of encapsulated CBZ against MDA-MB-231 and MCF-7 in targeted and non-targeted models (NANO-TMT-PEG-PCL-CBZ and NANO-PEG-PCL-CBZ, respectively) were investigated. As expected, NANO-TMT-PEG-PCL-CBZ displayed a significantly greater efficacy relative to NANO-PEG-PCL-CBZ ($p < 0.001$) at the concentration of 100 μM in MDA-MB-231 cells. In other words, NANO-TMT-PEG-PCL-CBZ was more effective to kill the highly metastatic cancer cells than NANO-PEG-PCL-CBZ. In contrast, NANO-TMT-PEG-PCL-CBZ showed no significant increase of the cytotoxicity as compared to non-targeted micelles in MCF-7 cells.

3.5. Cellular migration of MCF-7 cells

Fig. 7 illustrates a traditional scratch/wound healing assay evaluating MCF-7 cellular migration on TCPS. MCF-7 cells were cultured to confluence in serum-containing media on TCPS at the start of the experiment. After 48 h treatment with free CBZ, NANO-PEG-PCL, NANO-PEG-PCL-CBZ, and NANO-TMT-PEG-PCL-CBZ, cell migration is quantified by image analysis of five randomly selected fields of the denuded areas of triplicate experiments. The mean wound area is expressed as percent of wound area from three identically treated plates. After 48 h, only 71% of the scratch area remains in control group. However, using of polymeric micelles with and without (the presence) of CBZ and TMT result a significant increase ($p < 0.01$, $p < 0.01$, and $p < 0.001$, respectively) in the scratch area compared to control group. It is noteworthy that there is no significant difference between the percent of wound area in targeted (NANO-TMT-PEG-PCL-CBZ) and non-targeted nanomicelles (NANO-PEG-PCL-CBZ) groups (119% vs. 116%).

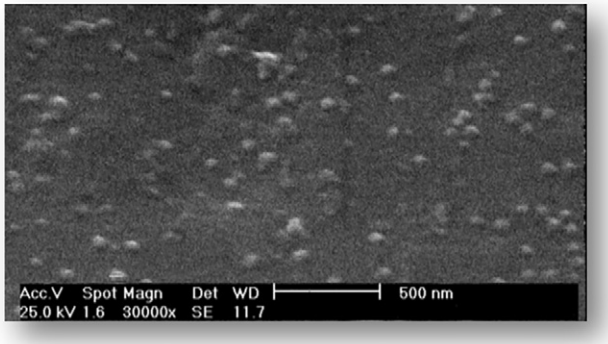

Fig. 4. SEM images of CBZ-loaded polymeric micelles.

3.6. Cellular migration of MDA-MB-231 cells

The impact of free CBZ, NANO-PEG-PCL, NANO-PEG-PCL-CBZ, and NANO-TMT-PEG-PCL-CBZ on MDA-MB-231 cell migration were examined by in vitro scratch assay in Fig. 8. When confluent monolayers of cells were treated with NANO-PEG-PCL, the MDA-MB-231 cells readily closed the gap over 48 h similar as the control group, whereas the treated cells with polymeric micelles containing 100 μM CBZ did not. In the wound-healing assay, encapsulated CBZ in (NANO-PEG-PCL and NANO-TMT-PEG-PCL) copolymer micelles caused a decrease in the number of cells migrating into the wound area in comparison to control group ($p < 0.001$). Moreover, in the group which were treated with NANO-TMT-PEG-PCL-CBZ, a large significant increase in percent of wound area was observed compared with NANO-PEG-PCL-CBZ group (70% vs. 42%, $p < 0.001$).

3.7. Apoptotic and necrotic cell death in MCF-7 cells

Flow cytometric assay was used to confirm the apoptotic and necrotic induction effect of encapsulated CBZ in copolymer micelles (NANO-PEG-PCL-CBZ, and NANO-TMT-PEG-PCL-CBZ) on MCF-7 cells. According to Fig. 9, the percentages of live cells in NANO-PEG-PCL-CBZ, and NANO-TMT-PEG-PCL-CBZ groups were 51% and 45%, respectively, which was significantly lower than that in control group (97%). Accordingly by using encapsulated CBZ (in copolymer micelles), a general risen the percentages of early and late apoptotic cells was observed in comparison to control group, but this increase was almost similar in targeted and non-targeted groups.

3.8. Apoptotic and necrotic cell death in MDA-MB-231 cells

The data presented in Fig. 10 show the effect of encapsulated CBZ in copolymer micelles (NANO-PEG-PCL-CBZ, and NANO-TMT-PEG-PCL-CBZ) on induction of apoptosis and necrosis in MDA-MB-231 cells by

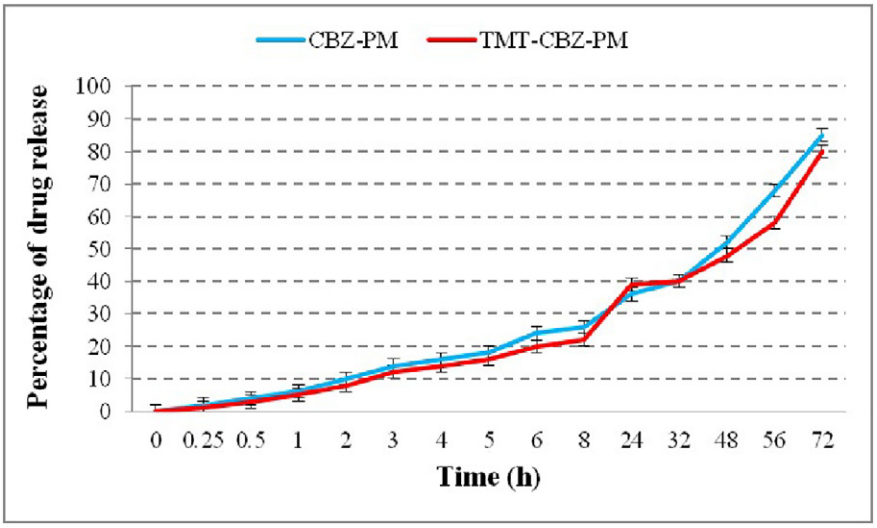

Fig. 5. In vitro release of cabazitaxel from non-targeted polymeric micelles and targeted polymeric micelles.

Flow Cytometry. As seen, treatment of cells with NANO-PEG-PCL-CBZ significantly increased the necrosis rate from 8% in the untreated, to 33% indicating that encapsulated CBZ proceeds cell death in MDA-MB-231 cells mainly through induction of necrosis. Moreover, the groups which were treated with NANO-TMT-PEG-PCL-CBZ showed apparent rise in the necrosis rate when compared to control group (65% vs. 8%) which was also noticeable in comparison to NANO-PEG-PCL-CBZ group (65% vs. 33%). Apart from necrosis, targeted encapsulated CBZ also increased the apoptosis rate from 0% to 16% indicating the treatment with targeted copolymer micelles exhibited greater apoptosis and necrosis induction than the non-targeted copolymer micelles (2.31-fold increase).

3.9. Uptake of coumarin-6-loaded micelles by MCF-7 and MDA-MB-231 cells

The cellular uptake characteristic of coumarin-6-loaded micelles was investigated qualitatively by confocal fluorescent microscopy (Fig. 11). The results shows that MCF-7 cells treated with either coumarin-6-loaded PEG-PCL or TMT-PEG -PCL NPs exhibited approximately the same fluorescent intensity of coumarin. In contrast, MDA-MB-231 cells treated with targeted (NANO-TMT-PEG-PCL) micelles exhibited a strong increase in the fluorescence intensity of coumarin in comparison to the cells treated with non-targeted (NANO-PEG-PCL) micelles ($p < 0.001$).

4. Discussion

In this study, synthesis of PEG-PCL was carried out through ring opening polymerization of ε-caprolactone using stannousoctoate as the catalyst. A similar process has been reported by Yuan et al., performing the reaction at a temperature of 140 °C for 24 h [18]. According to previous studies, it is confirmed that at reaction temperature of 110 °C and at reaction period of 24 h, sufficient conversion of ε-caprolactone to PCL occurs. Block copolymers were synthesized via amidation reaction between amine group of PCL and carboxylic acid end of PEG. For this purpose, EDC and NHS were applied for activation of the carboxyl group of PEG which was then reacted with NH_2-PEG. A number of methods have been previously reported for the self-assembly and micelle formation of block copolymers such as direct dissolution [24], solvent evaporation [25]or film formation and dialysis methods [26]. Each method can be applicable based on many factors such as particle size requirement, thermal and chemical stability of the active agent, reproducibility of the release kinetic profiles, and residual toxicity associated with the final product. By virtue of its simplicity and easily being scaled up, co-solvent evaporation method is generally recognized as an outstanding one, which has the potential for clinical application. Therefore, in this report, solvent evaporation method was applied for the preparation of micelles from PEG-PCL block copolymers. Micelles were characterized for their functional properties in drug delivery. A comparison between various studies on the preparation of PEG-PCL

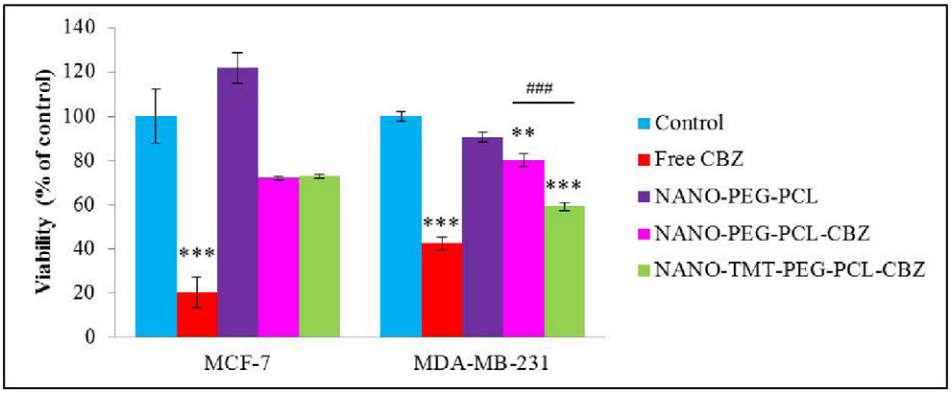

Fig. 6. In vitro cell cytotoxicity of free CBZ and CBZ encapsulated in NANO-PEG-PCL and NANO-TMT-PEG-PCL, (and NANO-PEG-PCL) block copolymer micelles against MCF-7 and MDA-MB-231 after 72 h incubation. Data are expressed as mean ± SEM of three independent experiments in duplicate. Difference between control and other groups is significant at $p < 0.01$ (**), $p < 0.001$ (***). Difference between targeted (NANO-TMT-PEG-PCL-CBZ) and non-targeted nanomicelles (NANO-PEG-PCL-CBZ) groups is significant at $p < 0.001$ (###).

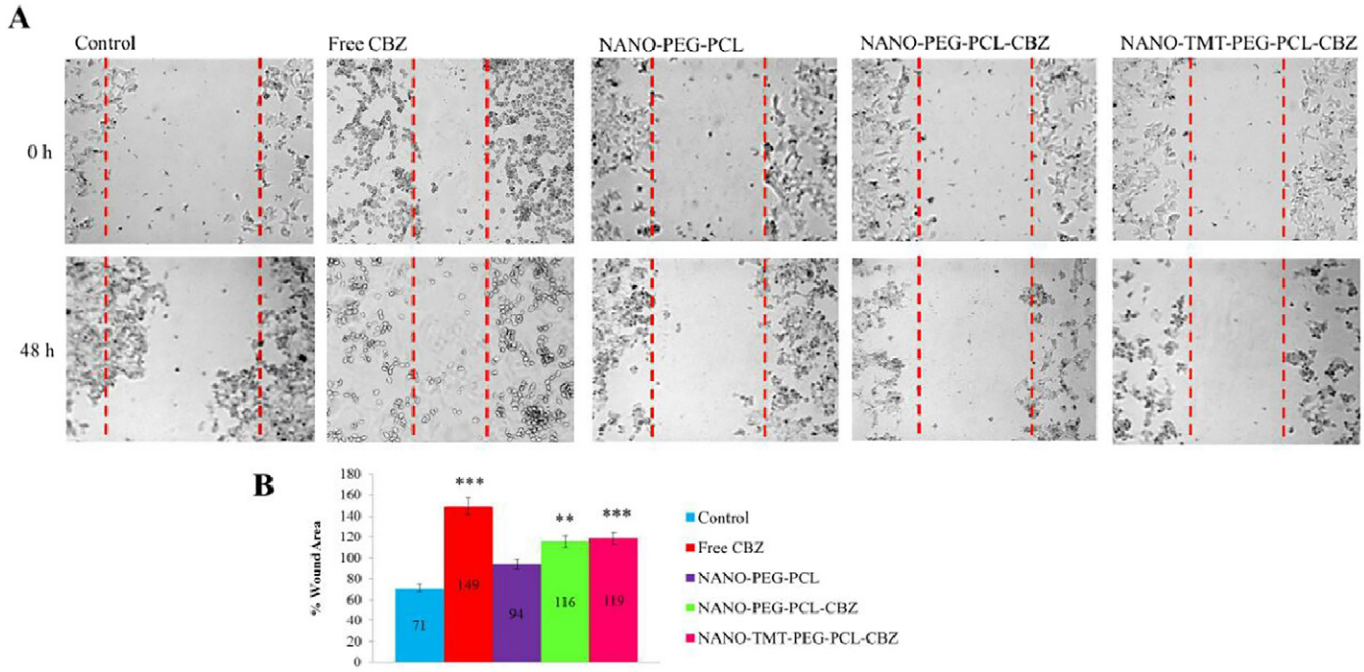

Fig. 7. (A) Determination of The effect of free CBZ, NANO-PEG-PCL, NANO-PEG-PCL-CBZ, and NANO-TMT-PEG-PCL-CBZ on MCF-7 cell migration by in vitro scratch assay. The cell monolayers were scraped and treated with different polymeric micelles with and without CBZ and peptide ligands (TMT). Cells were then photographed under an inverted microscope at 0 h and 48 h after scraping (4× magnification). The dotted lines define the areas lacking cells. (B) Quantification of cell migration according to percentage of wound area. Data are expressed as mean ± SEM of five randomly selected fields of the denuded areas of triplicate experiments. Difference between control and other groups is significant at $p < 0.01$ (**), $p < 0.001$ (***).

micelles demonstrates that aside from block copolymer molecular weight, other factors such as micellization procedure play a significant role in determining the average diameter and size distribution of the assembled nano-carriers. On the other hand, it is well established that the presence of hydrophilic PEG moieties around semi-crystalline PCL core leads to formation of stable micelles. In this study, CBZ-PM was fabricated by the co-solvent evaporation. In the co-solvent evaporation method, the block copolymer and the drug are dissolved in a volatile, water miscible organic solvent (selective co-solvent for the core-forming block). Self-assembly and drug entrapment is then triggered by the addition of water (non-solvent for the core-forming block) to the organic phase followed by the evaporation of the organic co-solvent.

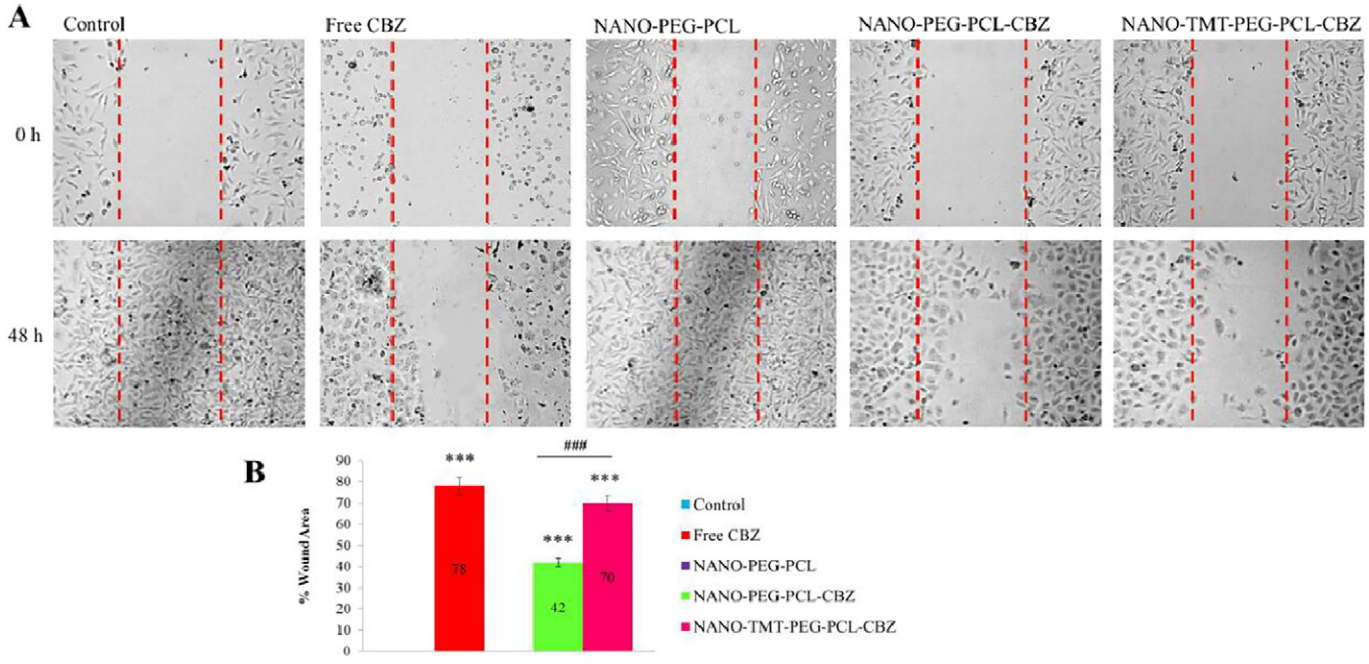

Fig. 8. (A) Determination of The effect of free CBZ, NANO-PEG-PCL, NANO-PEG-PCL-CBZ, and NANO-TMT-PEG-PCL-CBZ on MDA-MB-231 cell migration by in vitro scratch assay. The cell monolayers were scraped and treated with different polymeric micelles with and without CBZ and peptide ligands (TMT). Cells were then photographed under an inverted microscope at 0 h and 48 h after scraping (4× magnification). The dotted lines define the areas lacking cells. (B) Quantification of cell migration according to percentage of wound area. Data are expressed as mean ± SEM of five randomly selected fields of the denuded areas of triplicate experiments. Difference between control and other groups is significant at $p < 0.01$ (**), $p < 0.001$ (***).

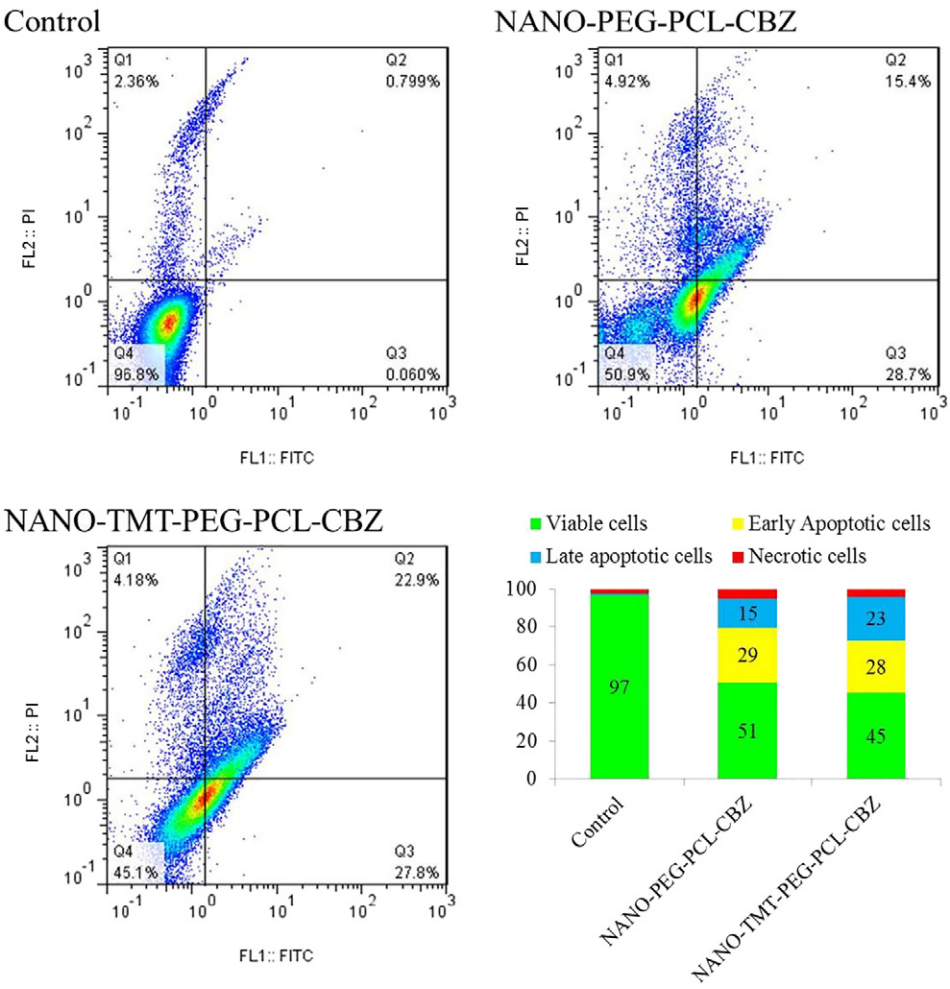

Fig. 9. Flow cytometric analyses of apoptosis and necrosis in MCF-7 cells induced by NANO-PEG-PCL-CBZ, and NANO-TMT-PEG-PCL-CBZ, using Annexin V-FITC and PI double staining. Quadrant analysis of fluorescence intensity of non-gated cells in FL1 (Annexin V) vs. FL2 (PI) channels was from 5000 events. The values shown in the lower left, lower right, upper left, and upper right quadrants of each panel represent the percentage of viable, apoptotic, necrotic, and late apoptotic (postapoptotic necrotic) cells, respectively.

The co-solvent evaporation method bears several advantages over dialysis method including more feasibility for scale up and less chance for drug loss during the encapsulation process. In the study carried out by Zhao et al., an enhanced micelle size and drug loading levels was observed in the self-assembled structures made from block copolymers with larger PCLs for encapsulation of a relatively large hydrophobic drug, cabazitaxel, into micelles by the aid of co-solvent evaporation method [27]. In that study, acetone was used as the organic co-solvent at an organic: aqueous phase ratio of 1:10. Herein, a systematic study determining the effect of co-solvent composition on carrier size, morphology and CBZ encapsulation has been conducted to achieve an optimum polymeric micellar carrier for the delivery of CBZ. Three important factors involved in the co-solvent evaporation method were determined as: the type of organic co-solvent, the volume fraction of organic to aqueous phase during the assembly process and the order of addition of the two phases (aqueous to organic phase or organic to aqueous phase). Each factor was individually manipulated and the effect of each alteration on carrier size, morphology and/or CBZ loaded levels was assessed. It has been reported that micelle with size in the nanoscale range (10–100 nm) can resist the systemic clearance by renal filtration and the reticuloendothelial system (RES) after administration [28]. The cytotoxicity of various CBZ formulations for metastatic and non-metastatic breast cancer cell lines (MCF-7 and MDA-MB-231) was shown in Fig. 1 and at least three facts were proved from the results. Firstly, the blank micelles were biocompatible since they showed no significant change in percentage of viability in comparison to control group in both cell lines. Secondly, the free CBZ was more cytotoxic than CBZ loaded in polymeric micelles (PM), likely because of its direct interaction with cells without fulfilling the release process. As a result, the highly hydrophobic free CBZ readily penetrated into the lipid membranes and then diffused into the cells leading to a greater extent of the cellular accumulation, which subsequently led to more cytotoxicity. It was demonstrated that CBZ has considerable antitumor activity against several cell lines, including those expressing the multidrug resistant gene (mdr-1) and other genes resistant to selected chemotherapeutic agents that is probably related to its poor affinity for p-glycoprotein [29]. Nevertheless, the highly effective delivery of CBZ is often hindered by their poor water solubility, which unfavorably may cause hypersensitivity, neurotoxicity, and other severe side effects with using ethanol, tween 80, or DMSO as a solvent [28]. In this regard, using polymeric micelles made of amphiphilic block copolymer such as PEG-PCL have emerged as powerful drug delivery vehicles with remarkable in vitro and in vivo success because of their biocompatible and antibiofouling characteristics [30]. Finally, decoration of polymeric micelles with the metastatic cancer-specific TMT ligand exhibited efficient anti-tumor effects in highly metastatic MBA-MD-231 cell line, but not in non-metastatic MCF-7 cell line in vitro.

In agreement with the results obtained with MTT assay, cell migration study showed that both CBZ-loaded PM and TMT-PM could stunt the cellular migration to a similar degree to each other in MCF-7 cells (Fig. 2). On the other hand, also flow cytometry results showed that targeted and non-targeted micelles have same apoptosis-inducing

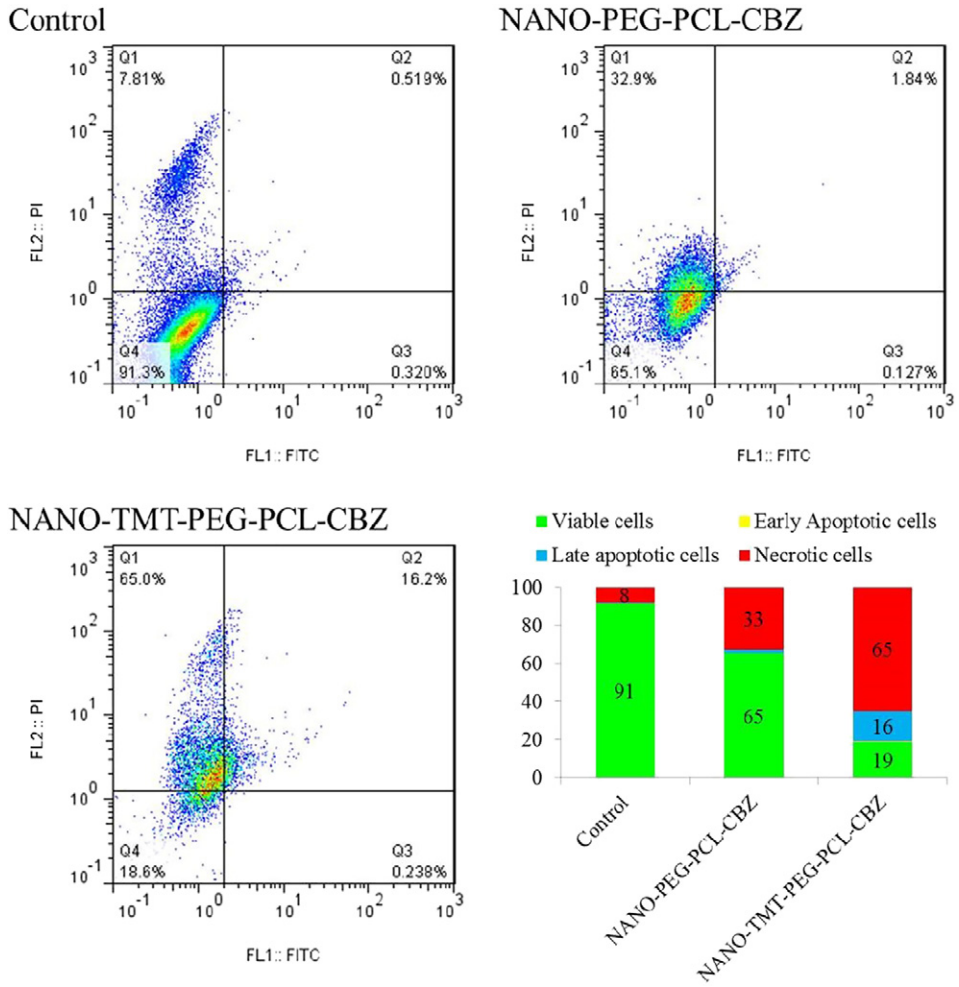

Fig. 10. Flow cytometric analyses of apoptosis and necrosis in MDA-MB-231 cells induced by NANO-PEG-PCL-CBZ, and NANO-TMT-PEG-PCL-CBZ, using Annexin V-FITC and PI double staining. Quadrant analysis of fluorescence intensity of non-gated cells in FL1 (Annexin V) vs. FL2 (PI) channels was from 5000 events. The values shown in the lower left, lower right, upper left, and upper right quadrants of each panel represent the percentage of viable, apoptotic, necrotic, and late apoptotic (postapoptotic necrotic) cells, respectively.

effects of CBZ on MCF-7 (Fig. 4). In this context, very low fluorescence was observed for both micellar formulations in MCF-7 cells and no visible difference was observed between these two systems, confirming that the enhanced uptake of TMT-polymeric micelles could be mediated by the TMT receptor, which expressed on the cellular surface of highly metastatic cancer cells MDA-MB-231, but not on the non-metastatic cell line MCF-7. In the following, since TMT-PM was developed to specifically target the highly metastatic cancer, we compared the specific cellular effects of PM and TMT-PM in MDA-MB-231 cancer cell line with metastatic potential. In cell migration analysis, it was observed that TMT-PEG-PCL-CBZ showed a significantly higher inhibitive effect on cell proliferation in comparison with PEG-PCL-CBZ at the same concentration of CBZ ($p < 0.001$). This revealed that the peptide modification could increase the delivery efficiency of antitumor drugs, which was supported by previous studies from others [31,32]. We next verified whether TMT-coupled PM affected tumor cell viability in coincident with their affinity to metastatic tumor cells. Accordingly, flow cytometry analysis displayed remarkable apoptosis (16%) and necrosis (65%) in MDA-MB-231 cells treated with TMT-PEG-PCL-CBZ, and moderately induced apoptosis (2%) and necrosis (33%) in PEG-PCL-CBZ treated MDA-MB-231 cells (Fig. 5). Obviously, a higher ratio of cell death was induced in active targeted group than that in passive targeted group for the same cell line, which supported that the presence of tumor cell-targeting ligands on polymeric micelles can mediate the binding and subsequent drug internalization into the tumor cells, resulting in elevated drug accumulation in the tumor and enhanced anticancer efficacy. We further observed cells treated with PM-CBZ exhibited very low fluorescence intensity, indicating its low non-specific cellular uptake. However, TMT-PM-CBZ demonstrated more green spots in MDA-MB-231 cell line, revealing the higher uptake in these cell lines than PM-CBZ as expected. Moreover, most of the visible fluorescence was observed in the cytoplasm compartment and it seemed that micelles did not enter the nuclei, in accordance with previous studies. In general, the above quantitative and qualitative studies consistently demonstrated that the TMT modification could markedly improve the specific recognition and uptake of the PM by highly metastatic breast tumor cells, probably due to the enhanced interaction of TMT—PM with receptors expressed on metastatic cancer cells.

5. Conclusions

In this work, cabazitaxel, as an approved efficient anticancer drug, was successfully loaded onto the nanosized polymeric micelles and then nanomicelles were conjugated to TMT peptide as targeting agent. The confocal microscopy results shows that MCF-7 cells treated with both targeted and non-targeted nanomicelles exhibited approximately the same fluorescent intensity. In contrast, MDA-MB-231 metastatic cancer cells treated with targeted nanomicelles exhibited a strong increase in the fluorescence intensity in comparison to the cells treated with non-targeted nanomicelles. Flow cytometry analysis displayed remarkable apoptosis (16%) and necrosis (65%) in MDA-MB-231 cells treated with targeted nanomicelles. Obviously, a higher ratio of cell

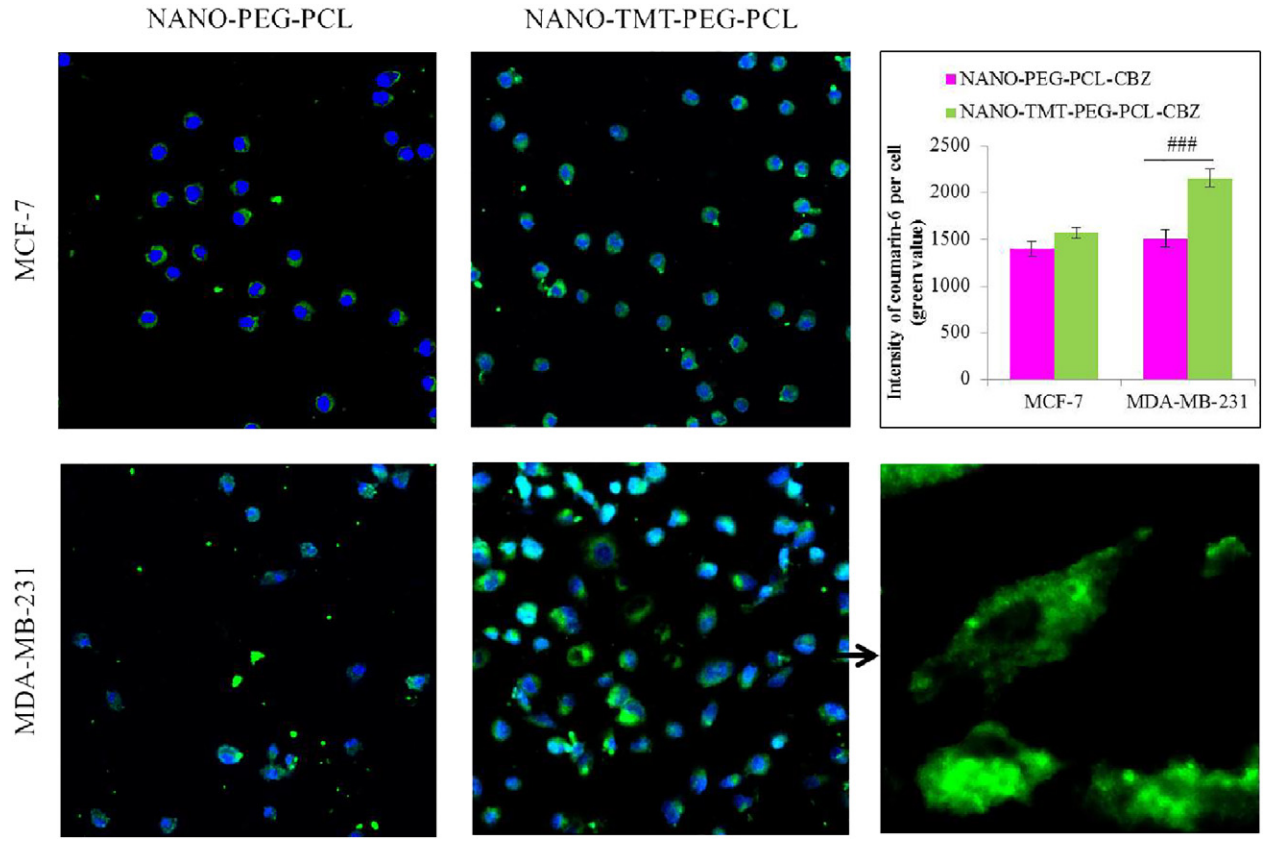

Fig. 11. Confocal images showing cellular uptake of coumarin-6-loaded PEG-PCL and TMT-PEG-PCL nanoparticles in two kinds of cancer cells, the nuclei are stained with DAPI. Images of the fields were acquired with a magnification of 20× and 100×. The graph shows quantification of the average fluorescence intensity of coumarin-6 per cell, i.e. the sum of green values of all pixels in the image divided by the number of nuclei. The error bars indicate SEM. Difference between targeted (NANO-TMT-PEG-PCL) and untargeted micelles (NANO-PEG-PCL) groups is significant at $p < 0.001$ ($^{###}$).

death was induced in active targeted group than that in passive targeted group for the same cell line. TMT modification could markedly improve the specific recognition and uptake of nanomicelles by highly metastatic breast tumor cells, probably due to the enhanced interaction with TMT receptors expressed on metastatic cancer cells.

Acknowledgments

This study was supported by a grant No. 9201-57-22033 from Tehran University of Medical Sciences.

References

[1] S. Oudard, TROPIC: phase III trial of cabazitaxel for the treatment of metastatic castration-resistant prostate cancer, Future Oncol. 7 (2011) 497–506.
[2] C.J. Paller, E.S. Antonarakis, Cabazitaxel: a novel second-line treatment for metastatic castration-resistant prostate cancer, Drug Des. Devel. Ther. 5 (2011) 117–124.
[3] G.S. Kwon, Polymeric micelles for delivery of poorly water-soluble compounds, Crit. Rev. Ther. Drug Carrier Syst. 20 (2003) 357–403.
[4] K. Temming, R.M. Schiffelers, G. Molema, R.J. Kok, RGD-based strategies for selective delivery of therapeutics and imaging agents to the tumour vasculature, Drug Resist. Updat. 8 (2005) 381–402.
[5] H. Otsuka, Y. Nagasaki, K. Kataoka, PEGylated nanoparticles for biological and pharmaceutical applications, Adv. Drug Deliv. Rev. 55 (2003) 403–419.
[6] V.P. Torchilin, Targeted polymeric micelles for delivery of poorly soluble drugs, Cell. Mol. Life Sci. 61 (2004) 2549–2559.
[7] R. Savic, L. Luo, A. Eisenberg, D. Maysinger, Micellar nanocontainers distribute to defined cytoplasmic organelles, Science 300 (2003) 615–618.
[8] V.P. Torchilin, A.N. Lukyanov, Z. Gao, B. Papahadjopoulos-Sternberg, Immunomicelles: targeted pharmaceutical carriers for poorly soluble drugs, Proc. Natl. Acad. Sci. USA 100 (2003) 6039–6044.
[9] O.H. Aina, R. Liu, J.L. Sutcliffe, J. Marik, C.X. Pan, K.S. Lam, From combinatorial chemistry to cancer-targeting peptides, Mol. Pharm. 4 (2007) 631–651.
[10] O.H. Aina, T.C. Sroka, M.L. Chen, K.S. Lam, Therapeutic cancer targeting peptides, Biopolymers 66 (2002) 184–199.
[11] W. Arap, R. Pasqualini, E. Ruoslahti, Cancer treatment by targeted drug delivery to tumor vasculature in a mouse model, Science 279 (1998) 377–380.
[12] X. Chen, C. Plasencia, Y. Hou, N. Neamati, Synthesis and biological evaluation of dimeric RGD peptide-paclitaxel conjugate as a model for integrin-targeted drug delivery, J. Med. Chem. 48 (2005) 1098–1106.
[13] S. Mukhopadhyay, C.M. Barnés, A. Haskel, S.M. Short, K.R. Barnes, S.J. Lippard, Conjugated platinum (IV)-peptide complexes for targeting angiogenic tumor vasculature, Bioconjug. Chem. 19 (2008) 39–49.
[14] X.B. Xiong, A. Mahmud, H. Uludağ, A. Lavasanifar, Conjugation of arginine-glycine-aspartic acid peptides to poly(ethylene oxide)-b-poly(epsilon-caprolactone) micelles for enhanced intracellular drug delivery to metastatic tumor cells, Biomacromolecules 8 (2007) 874–884.
[15] Z. Wang, Y. Yu, W. Dai, J. Lu, J. Cui, H. Wu, L. Yuan, H. Zhang, X. Wang, J. Wang, X. Zhang, Q. Zhang, The use of a tumor metastasis targeting peptide to deliver doxorubicin-containing liposomes to highly metastatic cancer, Biomaterials 33 (2012) 8451–8460.
[16] W. Yang, D. Luo, S. Wang, R. Wang, R. Chen, Y. Liu, TMTP1, a novel tumorhoming peptide specifically targeting metastasis, Clin. Cancer Res. 14 (17) (2008) 5494–5502.
[17] M.D. Galsky, A. Dritselis, P. Kirkpatrick, W.K. Oh, Cabazitaxel, Nat. Rev. Drug Discov. 9 (2010) 677–678.
[18] H.M. Aliabadi, S. Elhasi, A. Mahmud, R. Gulamhusein, P. Mahdipoor, A. Lavasanifar, Encapsulation of hydrophobic drugs in polymeric micelles through co solvent evaporation: the effect of solvent composition on micellar properties and drug loading, Int. J. Pharm. 329 (2007) 158–165.
[19] X. Wang, Y. Wang, X. Chen, J. Wang, X. Zhang, Q. Zhang, NGR-modified micelles enhance their interaction with CD13-overexpressing tumor and endothelial cells, J. Control. Release 139 (2009) 56–62.
[20] Y. Vachutinsky, M. Oba, K. Miyata, S. Hiki, M.R. Kano, N. Nishiyama, H. Koyama, K. Miyazono, K. Kataoka, Antiangiogenic gene therapy of experimental pancreatic tumor by sFlt-1 plasmid DNA carried by RGD-modified crosslinked polyplex micelles, J. Control. Release 149 (2011) 51–57.
[21] F. Esmaeili, M.H. Ghahremani, S.N. Ostad, F. Atyabi, M. Seyedabadi, M.R. Malekshahi, M. Amini, R. Dinarvand, Folate-receptor-targeted delivery of docetaxel nanoparticles prepared by PLGA-PEG-folate conjugate, J. Drug Target. 16 (2008) 415–423.
[22] Z. Hu, F. Luo, Y. Pan, C. Hou, L. Ren, J. Chen, J. Wang, Y. Zhang, Arg-Gly-Asp (RGD) peptide conjugated poly(lactic acid)-poly(ethylene oxide) micelle for targeted drug delivery, J. Biomed. Mater. Res. A 85 (2008) 797–807.

[23] M. Yuan, Y. Wang, X. Li, C. Xiong, X. Deng, Polymerization of lactides and lactones: 10. Synthesis, characterization, and application of amino terminated poly(ethylene glycol)-copoly(q-caprolactone) block copolymer, Macromolecules 33 (2000) 1613–1617.
[24] C. Allen, D. Maysinger, A. Eisenberg, Nano-engineering block copolymer aggregates for drug delivery, Colloids Surf. B: Biointerfaces 16 (1999) 3–27.
[25] H.M. Aliabadi, A. Mahmud, A.D. Sharifabadi, A. Lavasanifar, Micelles of methoxypoly(ethylene oxide)-b-poly(epsilon-caprolactone) as vehicles for the solubilization and controlled delivery of cyclosporine A, J. Control. Release 104 (2005) 301–311.
[26] C. Allen, J. Han, Y. Yu, D. Maysinger, A. Eisenberg, Polycaprolactone-b-poly(ethylene oxide) copolymer micelles as a delivery vehicle for dihydrotestosterone, J. Control. Release 63 (2000) 275–286.
[27] M.P. Bajgai, A. Santosh, C.P. Daman, K. Myung-Seob, R.L. Duck, Y.K. Hak, Synthesis characterization of brush copolymers based on methoxy poly (ethylene glycol) and poly (ε-caprolactone), J. Appl. Polym. Sci. 111 (2009) 1540–1548.
[28] O. Fernández, J. Afonso, S. Vázquez, B. Campos, M. Lázaro, L. León, L.M. AntónAparicio, Metastatic castration-resistant prostate cancer: changing landscape with cabazitaxel, Anti-Cancer Drugs 25 (2014) 237–243.
[29] R. Liu, L. Xi, D. Luo, X. Ma, W. Yang, Y. Xi, H. Wang, M. Qian, L. Fan, X. Xia, K. Li, D. Wang, J. Zhou, L. Meng, S. Wang, D. Ma, Enhanced targeted anticancer effects and inhibition of tumor metastasis by the TMTP1 compound peptide TMTP1-TAT-NBD, J. Control. Release 161 (2012) 893–902.
[30] Y. Song, Q. Tian, Z. Huang, D. Fan, Z. She, X. Liu, X. Cheng, B. Yu, Y. Deng, Self-assembled micelles of novel amphiphilic copolymer cholesterol-coupled F68 containing cabazitaxel as a drug delivery system, Int. J. Nanomedicine 9 (2014) 2307–2317.
[31] Z. Wang, Y. Yu, W. Dai, J. Cui, H. Wu, L. Yuan, H. Zhang, X. Wang, J. Wang, X. Zhang, Q. Zhang, A specific peptide ligand-modified lipid nanoparticle carrier for the inhibition of tumor metastasis growth, Biomaterials 34 (2013) 756–764.
[32] M. Shahin, S. Ahmed, K. Kaur, A. Lavasanifar, Decoration of polymeric micelles with cancer-specific peptide ligands for active targeting of paclitaxel, Biomaterials 32 (2011) 5123–5133.